Monte Carlo simulation of low-energy electron trajectories and energy loss in ZnS phosphor powders

ARTICLE *in* SURFACE AND INTERFACE ANALYSIS · JUNE 2001

Impact Factor: 1.25 · DOI: 10.1002/sia.1069

2 AUTHORS, INCLUDING:

H. C. Swart
University of the Free State
470 PUBLICATIONS **2,792** CITATIONS

SURFACE AND INTERFACE ANALYSIS
Surf. Interface Anal. 2001; **31**: 448–456

SIA

Monte Carlo simulation of low-energy electron trajectories and energy loss in ZnS phosphor powders

A. P. Greeff* and H. C. Swart

Department of Physics, University of the Free State PO Box 339, Bloemfontein, ZA-9300, South Africa

Received 6 November 2000; Revised 23 January 2001; Accepted 8 February 2001

During electron beam irradiation of ZnS phosphor powders, a non-luminescent ZnO layer is formed on the powder due to electron-beam-stimulated surface reactions. As the thickness of the oxide layer increases, the energy loss in the ZnS bulk decreases with a subsequent degradation in cathodoluminescence. Using the Monte Carlo technique, the trajectories of low-energy electrons were simulated in a ZnS phosphor powder with a ZnO overlayer of varying thickness based on recent models describing the energy loss and scattering angles of low-energy electrons in a solid. A diffusion interface between the ZnO layer and ZnS bulk was simulated by varying the concentration of O and S atoms in the interface. Modelling the interface in this way describes the electron trajectories and energy loss in the interface region, because a sharp interface between two dissimilar layers very seldom exists. In the energy-loss profiles the transition between ZnO and ZnS corresponds to a sharp increase in energy loss due to the increased rate of energy loss of electrons in ZnS. The diffusion interface has a smoothing effect on this sudden increase. From the electron trajectory data and corresponding energy loss, energy loss profiles were determined indicating the cumulative distribution of all the electron energy losses as a function of the interaction volume depth and thickness of the ZnO layer. When a distribution of incident angles is used, the profile differs from the typical energy-loss profile seen at normal incident angles. As the thickness of the ZnO layer increases, the total energy loss in the solid decreases due to the increase in the backscattering coefficient of electrons in ZnO. Copyright © 2001 John Wiley & Sons, Ltd.

KEYWORDS: ZnS-based phosphor; cathodoluminescence; Monte Carlo simulations; electron–solid interactions, scattering; diffusion interface

INTRODUCTION

The current trend in display technology is moving away from the old cathode ray tubes (CRTs) used in television and computer monitors towards the more compact full-colour flat panel displays (FPDs). One type of FPD that shows great promise is the field emission display (FED), with various companies already showing some high-voltage prototypes (see, for example: www.pixtech.com or www.candescent.com). It works on the same principle as a CRT, producing an image by cathodoluminescence (CL), but instead has millions of tiny metallic tips acting as electron emitters a few millimetres away from the phosphor screen. Using low-energy electrons it has a much lower power consumption than CRTs and, due to its compact set-up, can be made into thin, lightweight devices in unrestricted sizes. These are very important advantages, considering the current growth in the portable and hand-held electronic device market.

*Correspondence to: A. P. Greeff, Department of Physics, University of the Free State, PO Box 339, Bloemfontein, ZA-9300, South Africa. E-mail: petri@wwg3.uovs.ac.za
Contract/grant sponsor: National Research Foundation.

The question is whether or not conventional, highly efficient ZnS phosphors currently used in CRTs can be applied in the FED environment because the phosphors exhibit short lifetimes under these conditions. This is due to the degradation in CL when a non-luminescent ZnO layer forms on the surface of the ZnS phosphor according to the electron-stimulated surface chemical reaction (ESSCR) model.[1–3] The electron beam used to irradiate the powder dissociates the ambient H_2O gas or O_2 gas into atomic species that react with carbon on the surface to form volatile compounds and with ZnS to form a non-luminescent layer of ZnO with volatile SO_2. The advantage of lower power consumption in FEDs is also the main reason why these displays have not yet entered the market. At low energies (<5 keV) the electrons bombarding the phosphor screen have a much shorter penetration depth than those in CRTs. Because the generated CL is dependent upon the energy loss in the phosphor,[4,6] growth of the ZnO layer significantly influences the CL intensity, with energy lost in the non-luminescent ZnO layer not contributing to the CL.[7] In this paper a Monte Carlo electron trajectory simulation is used to determine an electron interaction volume and an energy loss profile through the ZnO layer and the ZnS bulk, with a diffusion interface between the oxide layer and the bulk.

DOI: 10.1002/sia.1069

By varying the thickness of the ZnO layer and the diffusion interface, the effect of these parameters on the energy-loss profile can be studied in detail.

THEORY

The Monte Carlo technique used to simulate electron trajectories in solids is well known and already reported elsewhere by various authors.[8–11] Therefore, only a brief outline based on the questions in the flowchart in Fig. 1 will be given here. An energetic electron penetrates a solid at an incident angle α and travels a certain distance S before it is scattered by an atom for the first time. In this step length the electron loses a certain amount of energy ΔE. Changing its trajectory, as shown in Fig. 2, the electron then travels another distance before it is scattered again. This process is repeated until the electron has lost all its energy to the solid. The simulation then is continued until a statistically significant result is obtained. By dividing the electron interaction volume into layers and calculating the energy loss in each of these layers, an energy-loss profile can be constructed. The scattering of the electron by an atom is viewed as an elastic scattering event with no energy loss but with a change in direction of the electron trajectory. The distance the electron moves between scattering events is viewed as an inelastic scattering event with a negligible direction change.

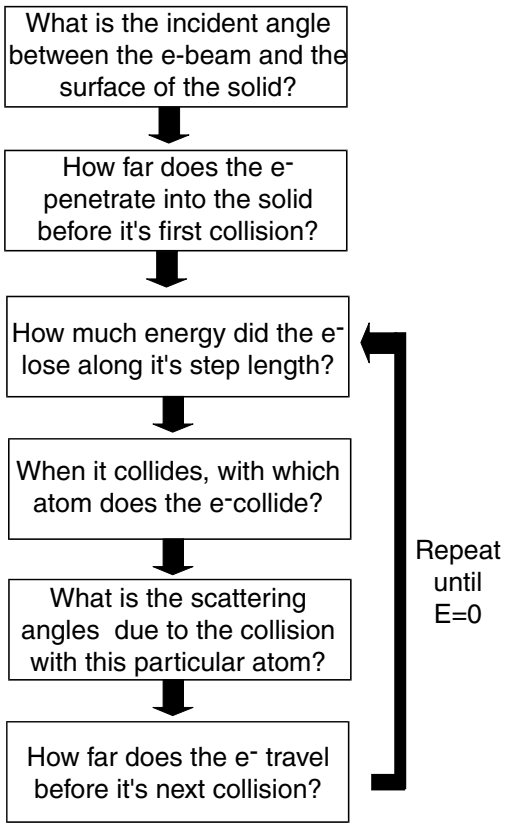

Figure 1. Set of questions to summarize the Monte Carlo technique used to simulate the trajectory of the single electron in a compound.

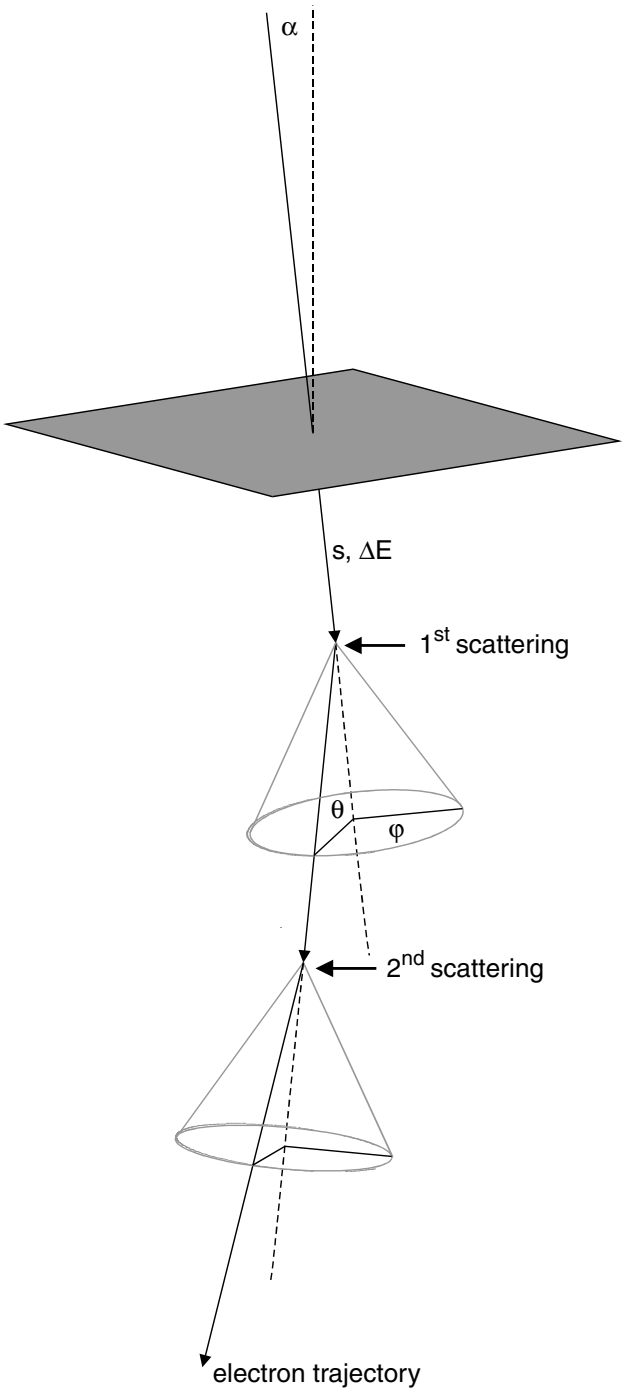

Figure 2. Graphical representation of the change in an electron's trajectory when it penetrates a solid at an incident angle and is scattered by the atoms of the solid.

Determining the electron incident angle

The incident angle of the electron is determined by the orientation of the electron beam with respect to the surface of the solid. The ZnS surface is not flat but consists of a distribution of flat and spherical-shaped particles. The electrons therefore do not strike the particle surface at normal incidence but at a distribution of incident angles between 0 and 90°. At other than normal incidence, the thickness of the non-luminescent ZnO layer in the direction of the beam is larger and varies with the incident angle.[7]

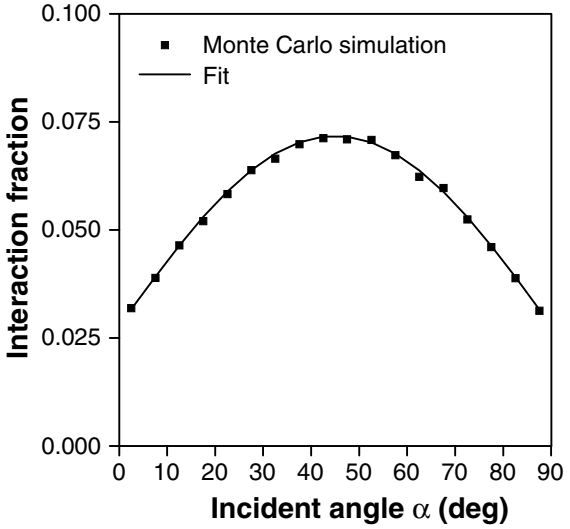

Figure 3. Results of a simulation to determine the distribution of electron beam incident angles. Equation (1) was fitted to the results to use as a probability density function in further Monte Carlo simulations.[12]

In determining the voltage dependence of the cathode ray efficiency of phosphor powders, Kinglsey and Prener[7] geometrically corrected for the morphology of the powder. We[12] determined the distribution of incident angles with a Monte Carlo technique and the results are shown in Fig. 3. The interaction fraction is a normalized value indicating the frequency of electron beam incident angles per interval of incident angle. The following equation

$$\cos(2\alpha) - \frac{2b\alpha}{a} = 1 - \left(2 + \frac{\mathrm{b}\pi}{\mathrm{a}}\right) P \tag{1}$$

where θ is the incident angle, a and b are fitting parameters and $R \in [0, 1]$, was fitted to the distribution in Fig. 3 and is used as a probability density function to sample possible incident angles using the Monte Carlo technique. The expression has no analytical solution and is solved using the Newton–Rhapson numerical iteration method.[13]

Electron step length

The depth that an electron penetrates into a solid before its first collision (i.e. its step length) is given by the expression[8]

$$S = -\lambda \ln(R) \tag{2}$$

where λ is the electron elastic mean free path and $R \in [0, 1]$. Equation (2) originates from the survival equation[14]

$$N/N_0 = \mathrm{e}^{-S/\lambda} \tag{3}$$

expressing the fraction of electrons N/N_0 left after it penetrated a distance S into the solid. This fraction can be represented by a random number R. The elastic mean free path for a compound is given by[10,11]

$$\lambda = \frac{1 \times 10^{-6}}{N_\mathrm{A}} \frac{\boldsymbol{CA}'}{\boldsymbol{F}\rho'} \boldsymbol{F}\sigma' \ (\mathrm{m}) \tag{4}$$

with $\boldsymbol{C}$ a row vector containing the atomic weight fraction of Zn, S and O. The column vector $\boldsymbol{A}'$ contains the atomic weight (g mol^{-1}) of the three elements. The atomic fraction $\boldsymbol{F}$ is again a row vector, whereas the density ρ' (g cm^{-3}) and the total elastic scattering cross-section σ'(m^2) are column vectors and N_A is Avogadro's number. The denominator $\boldsymbol{F}\sigma'$ refers to the total elastic scattering cross-section for the compound.[11] In the expression by Hovington *et al.*,[10] a mean density for the compound is used, but in Eqn. (4) this is modified to $\boldsymbol{F}\rho'$ to accommodate any changes in the stoichiometry of the solid. For a solid consisting of a single element, Eqn. (4) simplifies to that given by Newbury *et al.*[15] and Ding and Shimizu.[16]

In Fig. 4 the value of σ for Zn, S and O as a function of electron energy is shown. The value of σ is obtained from an elastic scattering cross-section database[17] and is discussed later in more detail. For all the elements the total scattering cross-section decreases with an increase in electron energy, with Zn (physically the largest atom) having the largest cross-section. Only at very low energies is the cross-section of O larger than that of Zn. By using Eqn. (4) the elastic mean free path of an electron in a compound can be calculated. In Fig. 5 the elastic mean free path for ZnO and ZnS is shown. In the diffusion interface the mean free path for a compound consisting of Zn, S and O also can be calculated using Eqn. (4). The varying concentration of these three elements will vary the elastic mean free path as a function of depth in the diffusion interface.

Electron energy loss

The energy loss ΔE of the electron along its step length is determined by multiplying its step length S by an energy-loss factor

$$\Delta E = \frac{\mathrm{d}E}{\mathrm{d}S} \times S \tag{5}$$

The most widely used analytical expression for the energy-loss factor has been that of Bethe (1930) and it gives

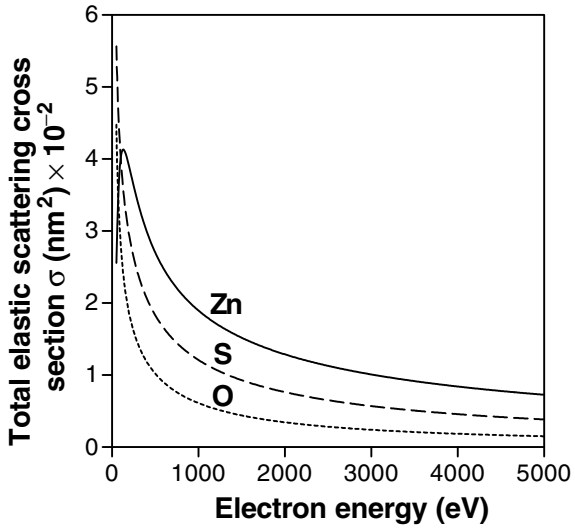

Figure 4. Total elastic scattering cross-section as a function of electron energy for Zn, S and O. The value for σ is obtained from a database supplied by NIST using the Mott theory describing elastic scattering.

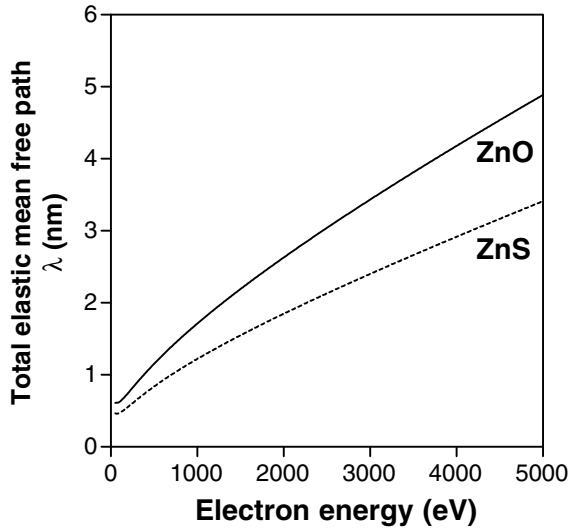

Figure 5. Elastic mean free path for ZnO and ZnS as a function of electron energy. In the diffusion interface, the total elastic mean free path is a linear combination of the individual mean free paths for the elements Zn, S and O based on the atomic concentration of each element (not shown here).

good results over a wide energy range. However, at low electron energies (<10 keV) certain events such as inner shell ionizations are no longer possible and the Bethe expression does not compensate for this. Writing the Bethe expression in a more generalized version, the total stopping power can be expressed as the sum of core ionizations and plasmon and conduction electron excitations,[18] with the number of terms reducing with a decrease in electron energy. Joy and Luo[19] suggested a modification to the mean ionization potential that represents the average energy loss per interaction by considering all possible energy-loss processes.[23] The mean ionization potential, which represents the summation of these terms, should be modified to be energy dependent. They showed that the modified expression is in good agreement with other theoretical models of Tung[20] and Rao-Sahib and Wittry.[21] The modified Bethe expression is given by

$$\frac{dE}{dS} = -\frac{7.85 \times 10^{12}}{E}\frac{\rho Z}{A}\ln\left(\frac{1.116E}{J^*}\right) \text{ (eV m}^{-1}\text{)} \quad (6)$$

where E is the electron energy (eV), F is the atomic fraction, ρ is the density (g cm^{-3}), Z is the atomic number, A is the atomic weight of a specific element and J^* is the modification suggested by Joy and Luo[22]

$$J^* = \frac{J}{1 + 0.85J/E} \quad (7)$$

where J is the mean ionization potential of the material

$$J = 9.76Z + 58.8Z^{-0.19} \text{ (eV) } Z \geq 13 \quad (8)$$

or

$$J = 11.5Z \text{ (eV) } Z \leq 12 \quad (9)$$

In a compound, the modified Bethe expression becomes[10]

$$\frac{dE}{dS} = \sum_{i=1}^{n} C_i\left(\frac{dE}{dS_i}\right) \text{ (eV m}^{-1}\text{)} \quad (10)$$

where n is the number of elements and C_i is the weight fraction of each element. To change the atomic fraction into a weight fraction, the following expression is used[24]

$$C_i = \frac{F_i A_i}{\boldsymbol{F}\boldsymbol{A}'} \quad (11)$$

where C_i is the weight fraction and F_i is the atomic fraction of each element i and $\boldsymbol{F}$ and $\boldsymbol{A}'$ are row and column vectors containing the atomic fraction and weight fraction of Zn, S and O, respectively.

In Fig. 6 the energy-loss rate of electrons due to screening from Zn, S and O atoms is shown as a function of electron energy. Because Zn is the larger atom, the screening effect is expected to be the most dramatic and to be responsible for the greatest electron energy loss over the whole range of electron energy values. The energy loss associated with S and O atoms again is based upon the size of the atoms.

Atoms responsible for scattering

In a compound, the decision on which an element's atom is responsible for scattering the electron is based upon the elemental contribution to the total elastic scattering cross-section of the solid.[11] In the particular case of ZnO/ZnS, for any given number $R \in [0,1]$ the Zn atoms are responsible for the scattering when

$$0 \leq R \leq \frac{F_{Zn}\sigma_{Zn}}{\boldsymbol{F}\sigma'} \quad (12)$$

or S atoms when

$$\frac{F_{Zn}\sigma_{Zn}}{\boldsymbol{F}\sigma'} \leq R \leq \frac{F_{Zn}\sigma_{Zn} + F_S\sigma_S}{\boldsymbol{F}\sigma'} \quad (13)$$

or O atoms when

$$\frac{F_{Zn}\sigma_{Zn} + F_S\sigma_S}{\boldsymbol{F}\sigma'} \leq R \leq 1 \quad (14)$$

where F_{Zn} and F_S are the atomic concentrations of Zn and S, respectively, and σ_{Zn} and σ_S are the total elastic scattering cross-sections of these two elements.

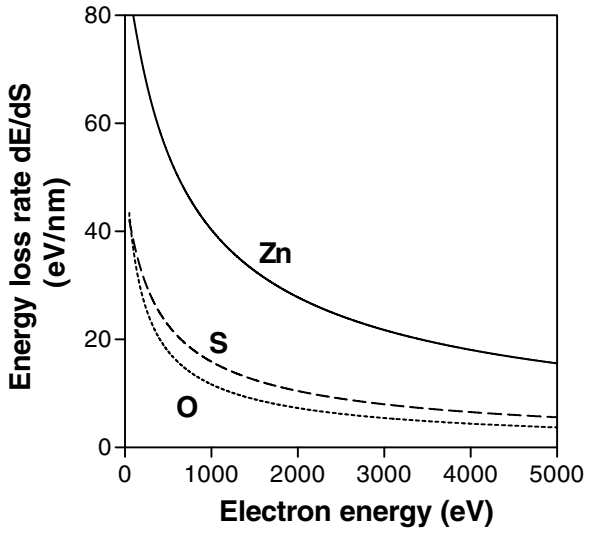

Figure 6. Rate of electron energy loss due to screening from Zn, S and O atoms according to Eqn. (6).

Depending upon the desired wavelength of light emitted during CL, ZnS powder is doped with specific trace elements. For example, to obtain blue light the phosphor powder is doped with Ag and Cl atoms, to obtain green light, the dopant atoms are Cu, Al and Au. Although these dopants are responsible for the light emission by forming recombination centres, their concentrations are minute and can be neglected for all practical reasons when simulating the electron trajectories.

By varying the concentration of the elements in the vector $\boldsymbol{F}$ according to an error function, it is possible to simulate the ZnO layer on top of the ZnS bulk with a diffusion layer between the two layers as shown in the simulated depth profile in Fig. 7.

Using the simulated depth profile in Fig. 7 to supply concentration values for $\boldsymbol{F}$ it is therefore possible to select the atom responsible for scattering based on its concentration at a particular depth. For example, at a depth of 10 nm (see Fig. 7) the concentration of Zn is 50% and that of S and O is 25%. Using these values, the scattering cross-section as a function of electron energy and Eqns (12)–(14), a graphical representation of the scattering frequency for Zn, S and O atoms as a function of electron energy is shown in Fig. 8. In the Monte Carlo code the element responsible for the scattering event at a certain electron energy is chosen based on the value of a randomly distributed number R. For example, if an electron has an energy of 2000 eV and the random number has a value of 0.5, then the Zn atom is responsible for the scattering event. At the same energies, the S atom acts as a scattering center if R has a value of 0.75 or the O atom if R has a value of 0.9. Considering that the distribution of values for R is randomly spread, Zn atoms will be responsible for the largest part of the scattering frequency, with S atoms second and O atoms third. This is due not only to a higher concentration of Zn but also to a larger cross-section, as seen in Fig. 4. At very low electron energies (<300 eV) the participation of Zn atoms decreases,

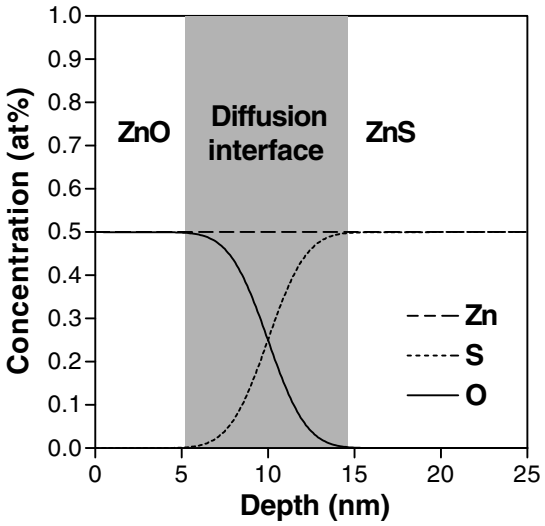

Figure 7. Simulated depth profile showing the atomic concentration as a function of depth for a 10 nm thick ZnO layer on top of ZnS. The diffusion interface has a total width of 10 nm.

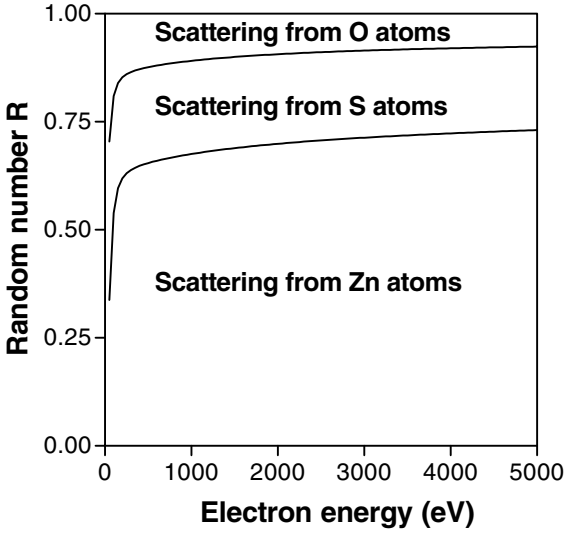

Figure 8. Graphical representation of the frequency of scattering from Zn, S and O atoms as a function of the electron energy corresponding to the concentration profile shown in Fig. 7.

whereas that of S and O atoms increases in the scattering frequency.

Scattering angles

Referring back to Fig. 2, the two scattering angles responsible for changing the electron trajectory are the azimuthal and polar angles ϕ and θ, respectively. The azimuthal angle is simply any angle between 0 and 360°, whereas the polar angle is a function of the differential elastic cross-section of the atom responsible for the scattering event.

In the Monte Carlo simulation, the elastic cross-section is used in two ways. As already seen, the total elastic cross-section is used to describe the mean free path between scattering events, whereas the differential elastic cross-section determines the polar scattering angle. A commonly used elastic scattering cross-section is the screened Rutherford cross-section, which has a convenient analytical form and is straightforward to implement in a Monte Carlo calculation. However, the screened Rutherford cross-section can be applied only to high-energy electrons and solids with a low atomic number. An alternative to the screened Rutherford cross-section is the partial wave expansion method of the Mott scattering cross-section.[25] These values are available from a database of the National Institute of Standards and Technology (NIST),[17] forming part of their standard reference data programme, and supplies the differential and total scattering cross-sections for elements with atomic numbers between 1 and 96 and for electron energies ranging from 50 eV to 10 keV.

In Fig. 9 the polar scattering angle is shown for oxygen as a function of the electron energy and a number between 0 and 1 according to values obtained from the NIST database. For all three elements Zn, S and O the scattering angle is quite small for the largest part of the energy range but increases considerably at very low electron energies.

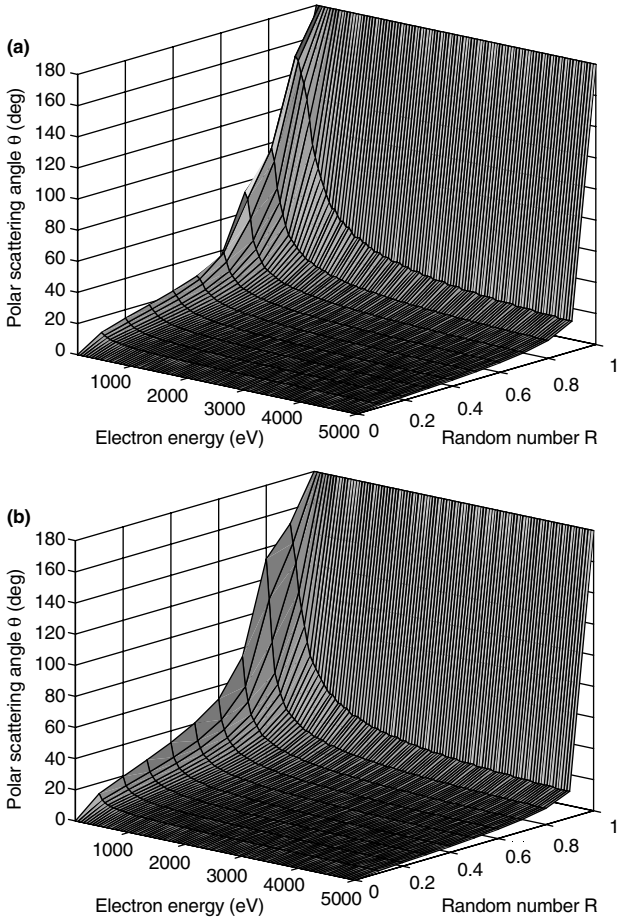

Figure 9. Polar scattering angles for (a) S atoms and (b) O atoms as a function of the electron energy and a random number provided by the NIST database.[17]

RESULTS

In Fig. 10 the Monte Carlo results are shown for simulating the trajectory of 100 electrons each with an initial energy of 2 keV through a 10 nm thick ZnO layer into the ZnS bulk. The shaded region represents the diffusion interface with a total thickness of 10 nm. The concentration of S and O above, in and below the diffusion interface varies according to the depth profile showed in Fig. 7 with the thickness of the ZnO layer taken at the depth where O decreased to 50% of its original concentration. The effect of using a distribution for the electron incident angle is evident in the general direction of the initial electron trajectories in the solid. The final trajectory of several backscattered electrons that left the sample is also visible on the surface. However, to obtain a reliable backscattering coefficient, the number of electrons should be increased by at least three orders of magnitude.

Contrary to the method employed by Hovington *et al.*,[10] no correction is made for the effect that the change in region from ZnO to ZnS has on the electron elastic mean free path and energy loss between scattering events. This is for two reasons: the transition between the two regions is not abrupt, but gradual due to the diffusion interface; and the electron step length between scattering events is short and the diffusion interface thick enough to accommodate this change in concentration when computing the step length and energy loss.

To determine an energy-loss profile through the interaction volume, the volume is divided up into a number of thin horizontal layers and the energy loss in each layer is determined, giving the total energy loss as a function of the depth of each layer. In Fig. 11 the simulated electron trajectories shown in Fig. 10 were used to determine a very low resolution energy-loss profile. Because the exact position of each scattering event and the electron's associated energy at that position are known, the energy-loss rate $\Delta E_z/\Delta z$ between two subsequent scattering events at depths z_i and z_{i+1} can be determined

$$\frac{\Delta E_z}{\Delta z} = \frac{E_i - E_{i+1}}{z_i - z_{i+1}} \tag{15}$$

Dividing the interaction volume into many layers, each 0.1 nm thick, this energy loss is then spread through these layers between depths z_i and z_{i+1}. In Fig. 11 each of these layers were 10 nm thick, leading to a very rough approximation of the energy-loss profile. The y-axis of the energy-loss graph is expressed as the unitless fractional energy loss. This term expresses the energy loss of electrons $\Delta E/\Delta z$ [refer to Eqn. (15)] in the solid as a fraction of the total input energy, which in this case was 200 keV (2 keV/electron × 100 electrons). The sum total of all the fractional energy losses in the layers is 0.73 (146 keV/200 keV), indicating that some still-energetic electrons were backscattered. This is confirmed by a backscattering coefficient of 0.3, indicating that ~30% of electrons left the sample. This value is obtained by monitoring the number of electrons that are scattered to such an extent during the simulation that it exists the sample again.

In Fig. 12 the energy-loss profile is shown for a diffused 10 nm thick ZnO layer on top of the ZnS bulk. The thickness value was chosen according to previous measurements by XPS depth profiles on degraded ZnS phosphor powders.[5] This profile was obtained by simulating 10^5 trajectories of 2 keV electrons and using Eqn. (15) to determine the energy loss. Figure 12 differs from the energy-loss profiles shown by Toth and Phillips[6] for 4–20 keV electron beams in GaAs. In the profiles of Toth and Phillips the energy loss increases from zero at the surface to a maximum value at some depth below the surface before it then decreases to zero. The energy-loss profiles were calculated by dividing the solid into a number of horizontal layers, in the same way as described earlier. The simulation by Toth and Phillips was performed at a zero incident angle and therefore the initial electron trajectory is perpendicular to the layers. The energy loss during the first step length is spread over a large number of layers, minimizing the energy loss in each layer.

The direction of the electron changes only after the first scattering event. The electron trajectory is not perpendicular to the surface after the first scattering event and so the energy loss in the following step length is spread over a smaller number of layers, increasing the energy loss in each layer. In the following scattering events, the change in direction is more dramatic, increasing the effect.

The observed maximum energy loss at a depth of ~13 nm should not be confused with the above-mentioned maximum

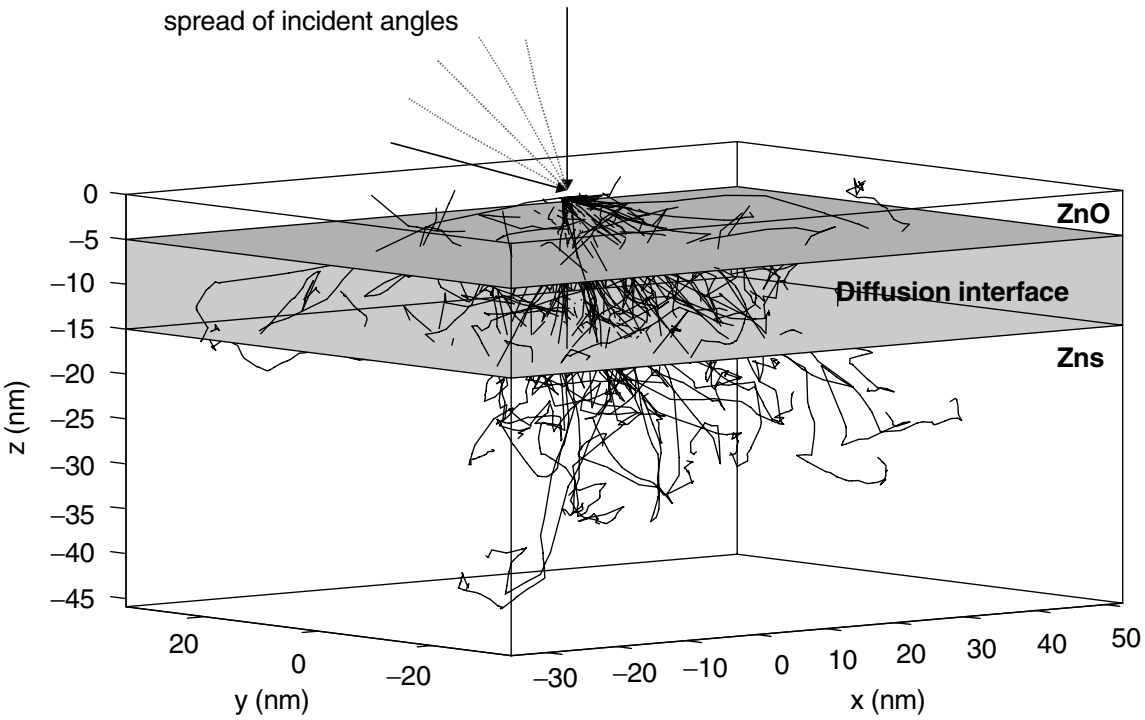

Figure 10. Monte Carlo simulation of 100 electron trajectories with an initial 2 keV energy. The shaded region represents the diffusion interface between the ZnO layer and the ZnS bulk. The concentration of Zn, S and O follows that of the simulated depth profile shown in Fig. 7, with the 50% mark of O at a depth of 10 nm.

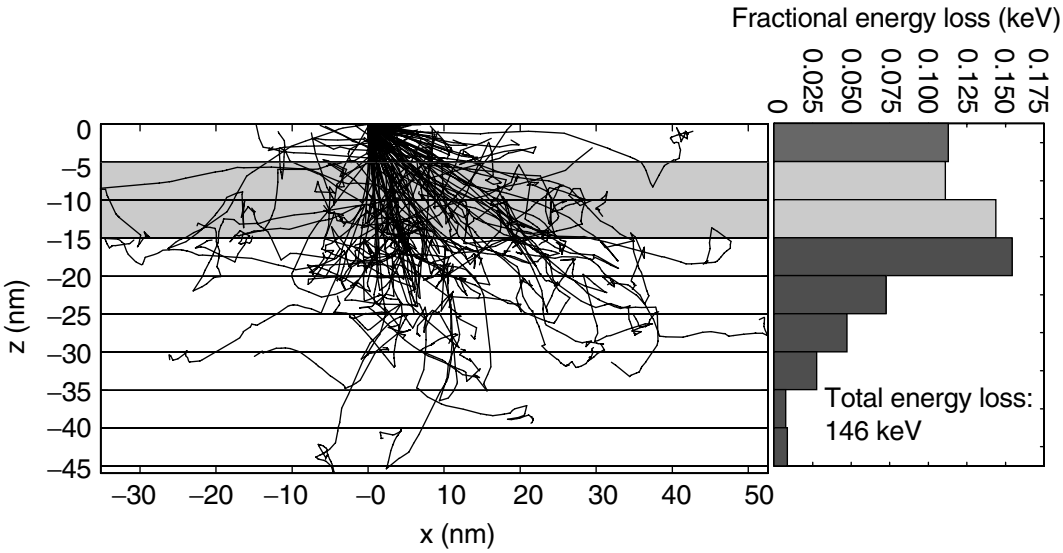

Figure 11. Energy-loss profile alongside the electron trajectories shown in Fig. 10, generated by dividing the interaction volume into horizontal layers and calculating the total energy loss in each layer. The shaded regions in the trajectory plot and corresponding energy-loss profile indicate the diffusion interface region.

energy loss as seen in Fig. 12. The maximum is due to the ZnO/ZnS interface and is attributed to the difference in electron energy loss associated with O and S atoms. In this profile the energy loss immediately starts to decrease from 0.0015 as a result of the distribution of incident angles used in the simulation. The initial electron trajectory is not perpendicular and therefore the energy loss during the first few step lengths is spread over a smaller number of layers, increasing the energy loss in these shallow layers. This masks the observed maximum seen in the energy-loss profiles of Toth and Phillips. A simulation that was performed with the same parameters as above, except that the incident angle was set to 0°, is shown as inset A in Fig. 12. The results are in agreement with those of Toth and Phillips. The importance of the distribution of the electron beam's incident angle must be stressed again.

Integrating the energy losses in Fig. 12 along the total depth gives a value of 0.5496, indicating that only about half of the initial electron energy is deposited into the solid. This also correlates with a measured backscattering coefficient of

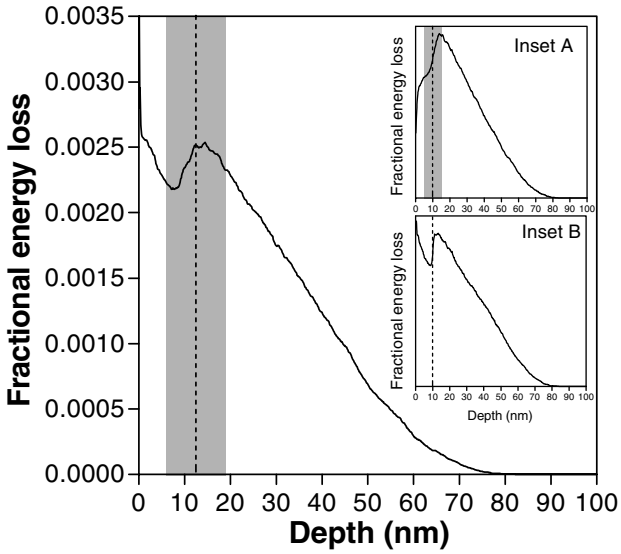

Figure 12. Simulated 2 keV energy-loss profile for a 10 nm thick ZnO layer on top of ZnS. The diffusion interface between ZnO and ZnS is 10 nm thick and indicated by the shaded area. In inset A a similar energy-loss profile is shown, but instead of using a distribution of incident angles (see text) a 0° incident angle was used. In inset B an energy-loss profile is shown without the diffusion interface.

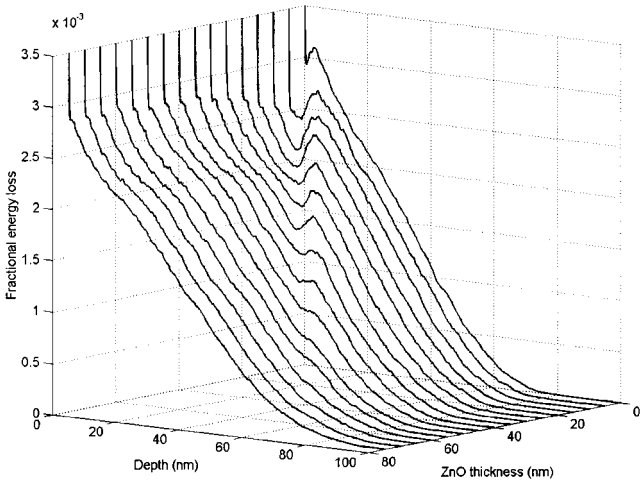

Figure 13. Simulated 2 keV energy-loss profiles as a function of ZnO thickness. The diffusion interface was 10 nm thick.

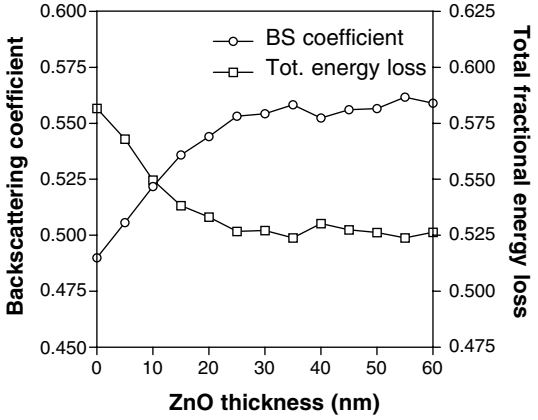

Figure 14. Comparison between the backscattering coefficient and total energy loss as a function of the ZnO thickness: (○) backscattering coefficient; (□) total energy loss.

0.5218, indicating that >50% of the still-energetic backscattering electrons left the solid after undergoing scattering events. The relatively high backscattering coefficient again can be attributed to the distribution of incident angles given by Eqn. (1).

The diffusion barrier (indicated by the shaded area in the graph) has a total width of 10 nm, with the concentration of Zn, S and O in this area corresponding to the profile shown in Fig. 7. The effect that the absence of such a diffusion barrier has on the energy-loss profile is shown in inset B in Fig. 12, with the profile increasing much more abruptly in the ZnO/ZnS region. Because the concentration of the Zn atoms remains constant in both regions, the increase should be due to the transition from O atoms in the ZnO layer to S atoms in the ZnS bulk. Referring back to Fig. 6, O oxygen has a lower rate of energy loss dE/dS than sulphur and therefore less energy is deposited into the layers when electrons travel through ZnO than when it travels through ZnS. Adding a diffusion barrier smooths out this transition from O to S atoms, resulting in a more gradual increase in the energy loss of the electrons in this region.

In Fig. 13 a collection of energy-loss profiles is shown for increasing ZnO thicknesses. The interface width was kept constant at 10 nm. The effect of increasing oxide thickness on the energy-loss profile is evident from the movement of the transition region between ZnO and ZnS to higher values on the depth scale. Although there is a slight increase in the electron range from the ZnS bulk to the ZnO layer, the area underneath each profile, which represents total energy loss, decreases with an increase in the ZnO thickness. In Fig. 14 the backscattering coefficient and total energy loss as a function of the ZnO thickness are compared. The correlation between these two parameters is clear from the trend displayed in the graph. As the thickness of this layer increases the backscattering coefficient increases and therefore more of the still-energetic electrons leave the sample and less energy is deposited into the solid, confirming the decrease in energy loss with increase in ZnO thickness. Comparing the polar scattering angles of O and S atoms (shown in Fig. 9) at very low energies (<1000 eV), O atoms have a larger polar scattering angle and therefore ZnO has a higher probability of contributing towards backscattered electrons. When the thickness of the ZnO layer exceeds the maximum penetration depth of the 2 keV electrons, the backscattering coefficient and total energy loss levels off.

Future work will focus on using these energy-loss profiles to model the CL generated during growth of the ZnO layer. Because the rate of electron energy loss determines the rate of electron–hole pair production, it can be assumed that the CL intensity generated in the solid is proportional to this energy loss. Because the ZnO layer is non-luminescent, is does not contribute towards CL generation and therefore that particular part of the energy-loss profile can be disregarded. The rest of the profile then is used as a basis to describe the pair production, recombination, photon generation and absorption.

CONCLUSIONS

(1) The electron energy loss in a diffusion interface between the ZnO layer and ZnS bulk was simulated by varying the concentration of O and S atoms in the interface in the Monte Carlo simulation. Modelling the interface in such a way provides a better physical model to describe the electron trajectories and energy loss in the interface region, because a sharp interface between two layers very seldom exists.
(2) In the energy-loss profile the transition between ZnO and ZnS corresponds to a sharp increase in energy loss, due to the increased rate of energy loss of electrons in ZnS. The diffusion interface has the effect of smoothing out this sudden increase.
(3) From the electron trajectory data and corresponding energy loss, energy-loss profiles were determined indicating the cumulative distribution of all the electron energy losses as a function of the interaction volume depth and thickness of the ZnO layer.
(4) The energy-loss profile is greatly influenced by the incident angle of the electron beam. When a distribution of incident angles are used, the profile differs from the typical energy-loss profile seen at normal incident angles.
(5) As the thickness of the ZnO layer increases, the total energy loss in the solid decreases due to the increase in the backscattering coefficient of electrons in ZnO.

Acknowledgement
The financial support of the National Research Foundation (NRF) is greatly appreciated.

REFERENCES

1. Swart HC, Sebastian JS, Trottier TA, Jones SL, Holloway PH. *J. Vac. Sci. Technol. A* 1996; **14**: 1697.
2. Oosthuizen L, Swart HC, Viljoen PE, Holloway PH, Berning GLP. *Appl. Surf. Sci.* 1997; **120**: 9.
3. Holloway PH, Trottier TA, Sebastian JS, Jones SL, Zhang X-M, Bang J-S, Abrams B, Thomes WJ, Kim T-J. *J. Appl. Phys.* 2000; **88**: 483.
4. Myhajlenko S. In *Luminescence of solids* (1st edn), Vij DR (ed.). Plenum Press: New York, 1998; 135.
5. Swart HC, Greeff AP, Holloway PH, Berning GLP. *Appl. Surf. Sci.* 1999; **140**: 63.
6. Toth M, Phillips MR. *Scanning* 1998; **20**: 425.
7. Kingsley JD, Prener JS. *J. Appl. Phys.* 1972; **43**: 3073.
8. Shimizu R, Ding Z-J. *Rep. Prog. Phys.* 1992; **55**: 487.
9. Reimer L, Stelter D. *Scanning* 1986; **8**: 265.
10. Hovington P, Drouin D, Gauvin R. *Scanning* 1997; **19**: 1.
11. Howell PGT, Boyde A. *Scanning* 1998; **20**: 45.
12. Greeff AP, Swart HC. *Surf. Interface Anal.* 2000; **29**: 807.
13. Burden RL, Faires JD. *Numerical Analysis* (5th edn). PWS Publishing: Boston, 1993; 56.
14. Sears FW, Salinger GL. *Thermodynamics, Kinetic Theory, and Statistical Thermodynamics* (3rd edn). Addison-Wesley: London, 1986; 281.
15. Newbury DE, Joy DC, Echlin P, Fiori CE, Goldstein JI. *Advanced Scanning Electron Microscopy and X-Ray Microanalysis* (1st edn). Plenum Press: New York, 1986; 4.
16. Ding Z-J, Shimizu R. *Scanning* 1996; **18**: 92.
17. *NIST Elastic Electron Scattering Cross Section Database*, Standard Reference Data Program, Database 64. National Institute of Standards and Technology: Gaithersburg, 1996.
18. Shimizu R, Ichimura S. *Toyota Foundation Research Report No. I-006*. Toyota Foundation: Tokyo, 1981.
19. Joy DC, Luo S. *Scanning* 1989; **11**: 176.
20. Tung CJ, Ashley JC, Ritchie RH. *Surf. Sci.* 1979; **427**: 427.
21. Rao-Sahib TS, Wittry DB. *J. Appl. Phys.* 1974; **45**: 5060.
22. Joy DC, Luo S, Gauvin R, Hovington P, Evans N. *Scanning Microscopy* 1996; **10**: 653.
23. Berger MJ, Seltzer SM. *Studies in Penetration of Charged Particles in Matter*, Nuclear Science Series Report No. 39, NAS-NRC Publication No 1133. National Academy of Science: Washington DC, 1964; 205.
24. Askeland DR. *The Science and Engineering of Materials*, (3rd SI edn). Chapman and Hall: London, 1996; 265.
25. Browning R, Eimori T, Traut EP, Chui B, Pease FW. *J. Vac. Sci. Technol. B* 1991; **9**: 3578.
26. Czyzewski Z, MacCallum DO, Romig A, Joy DC. *J. Appl. Phys.* 1990; **68**: 3066.